Metal Artifact Reduction Sequence: Early Clinical Applications[1]

Randall V. Olsen, MD • Peter L. Munk, MD • Mark J. Lee, BSc • Dennis L. Janzen, MD • Alex L. MacKay, PhD • Qing-San Xiang, PhD • Bassam Masri, MD

Artifact arising from metal hardware remains a significant problem in orthopedic magnetic resonance imaging. The metal artifact reduction sequence (MARS) reduces the size and intensity of susceptibility artifacts from magnetic field distortion. The sequence, which is based on view angle tilting in combination with increased gradient strength, can be conveniently used in conjunction with any spin-echo sequence and requires no additional imaging time. In patients with persistent pain after femoral neck fracture, the MARS technique allows visualization of marrow adjacent to hip screws, thus enabling diagnosis or exclusion of avascular necrosis. Other applications in the hip include assessment of periprosthetic soft tissues after hip joint replacement surgery, postoperative assessment after resection of bone tumors and reconstruction, and localization of unopacified methyl methacrylate cement prior to hip arthroplasty revision surgery. In the knee, the MARS technique allows visualization of structures adjacent to implanted metal staples, pins, or screws. The technique can significantly improve visualization of periprosthetic bone and soft-tissue structures even in patients who have undergone total knee arthroplasty. In patients with spinal fixation hardware, the MARS technique frequently allows visualization of the vertebral bodies and spinal canal contents. The technique can be helpful after wrist fusion or screw fixation of scaphoid fractures.
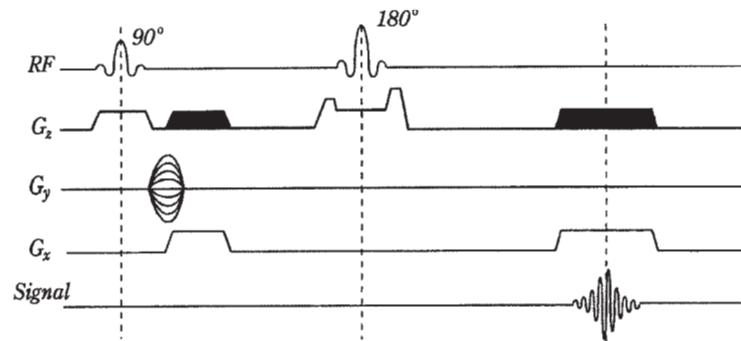
Figure 1.   Diagram of a conventional spin-echo sequence modified for the MARS technique. G_x = frequency-encoding gradient, G_y = phase-encoding gradient, G_z = section-selection gradient, RF = radio frequency.

Introduction

Since the inception of magnetic resonance (MR) imaging, the presence of metal in an anatomic area of interest has proved a difficult and annoying problem for musculoskeletal radiologists. Metal produces both a large area of signal void and extensive distortion around the implant (1–6). In most instances, the signal void and distortion preclude acquisition of useful information in the immediate area of the metallic object. Unfortunately, the presence of metal also degrades computed tomographic (CT) studies; thus, when metal is present in a patient, it has been impossible to obtain useful information. For this reason, many efforts have been made to minimize metal artifact by various investigators with only modest results (2,5–15).
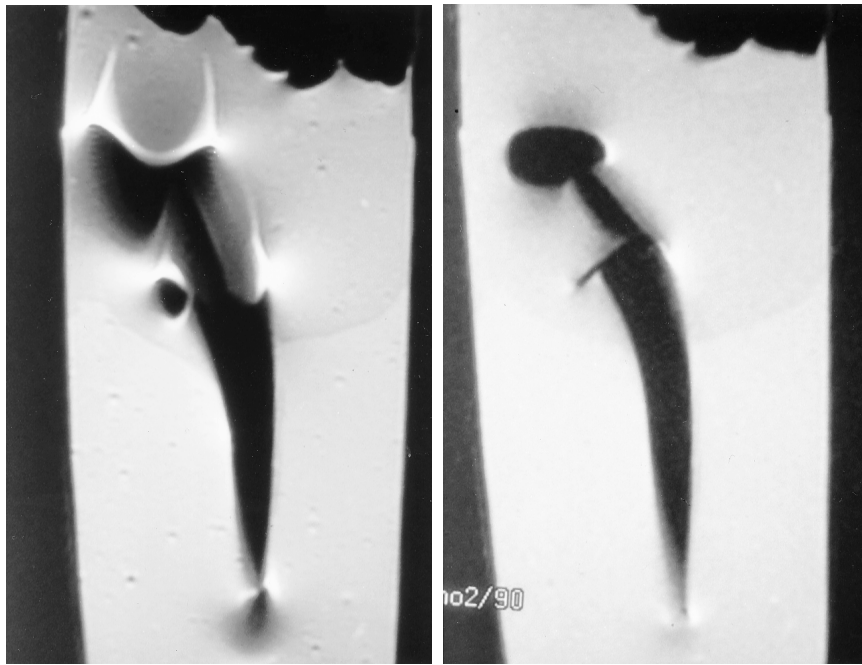
We have developed an MR imaging pulse sequence designed to reduce susceptibility artifacts arising from orthopedic hardware. This technique results in improved image quality and reduction of susceptibility artifact without an increase in imaging time. The technique frequently allows improved visualization of structures adjacent to the hardware and often yields diagnostically useful information (16–18). In this article, a description of the technique, clinical experience with the technique, and the current status of the technique are presented.

Description of Technique

There are at least two problems with imaging in the presence of susceptibility-induced field gradients caused by metal implants (1,6,16,19). First, the section is distorted from the ideal planar sheet. Second, there are geometric image distortions along the frequency axis due to the inhomogeneous field.

The metal artifact reduction sequence (MARS) was optimized for reduction of metal artifact by using the following three strategies (17,18). First, the section-selection gradient and radio-frequency bandwidth were increased by 17%, and a relatively narrow (3- or 4-mm) section thickness was used. Second, the read gradient was increased. The frequency bandwidth was 31.25 kHz for a 16-cm field of view (FOV) and 62.5 kHz for a 30-cm FOV. Third, view angle tilting was employed. The view

a.   b.

Figure 2.   Phantom study of a femoral component from total hip arthroplasty with a titanium alloy. The component was suspended in grease. **(a)** Coronal T1-weighted spin-echo MR image (repetition time msec/echo time msec = 500/15, 3-mm section thickness, 1.5-mm gap, 30-cm FOV) shows extensive distortion and artifact of mixed high and low signal intensity, especially around the proximal portion of the component. **(b)** Corresponding MR image obtained with the MARS technique shows some residual distortion, especially around the femoral head. However, a dramatic reduction in artifact is apparent, and the remaining signal void is now easily recognized as representing a femoral component.

angle was 34° for the 16-cm FOV and 32° for the 30-cm FOV. Each of these three strategies contributes about equally to reduction of metal artifact. The MARS technique is presented schematically in Figure 1, and its effectiveness in reducing susceptibility artifacts is illustrated in Figure 2. The aim of the first two strategies is to make the imaging gradients as large as possible relative to the susceptibility-induced gradients produced in the tissue by the metal implants. Increasing the section-selection gradient decreases section curvature. Increasing the frequency-encoding gradient decreases geometric distortion in the image. However, the increase in the frequency-encoding

gradient requires a larger image bandwidth, resulting in a decrease in signal-to-noise ratio. The signal-to-noise ratios for MARS images obtained with 16- and 30-cm FOVs were 29% and 50% lower, respectively, than that of conventional MR images, which had a frequency bandwidth of 16 kHz.

View angle tilting removes geometric distortion in the image by application of the section-selection gradient during the signal readout (19). It can be appreciated simply by realizing that, at the time of section selection, all the spins in the section precess within the same narrow frequency band determined by the frequency profile of the radio-frequency pulse. When the section-selection gradient is applied later during data acquisition, the spins will possess the same narrow frequency band (with frequency encoding ignored and in the absence of motion). Therefore, the resulting image is devoid of distortion due to inhomogeneous magnetic fields. However, tilting of the view angle results in blurring. The extent of this blurring was 2.7 mm for the 16-cm FOV and 2.5 mm for the 30-cm FOV.

In effect, nearby metal produces a chronic frequency shift from that imparted by the nominal imaging gradients. If a single-axis frequency-encoding gradient were applied (ie, no tilt), this chronic frequency shift would produce an apparent spatial shift of affected spins along the frequency-encoding axis. Use of a stronger frequency-encoding gradient reduces this spatial shift but does not remove it. The application of an additional gradient along the section-selection direction with the same amplitude as the section-selection gradient restores spins in the radio-frequency–selected volume to the same band of frequencies, thus compensating for the chronic metal-indu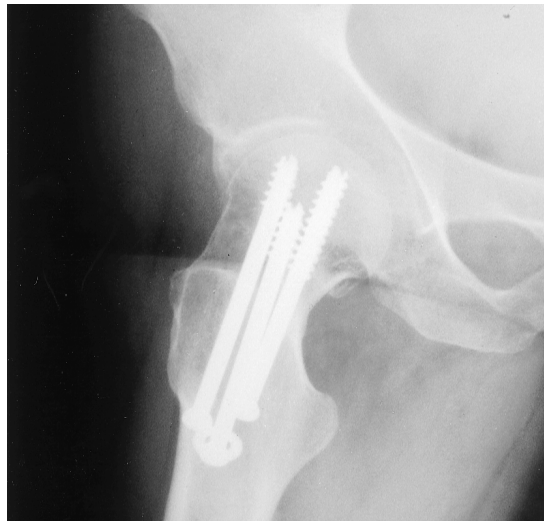ced frequency shift. Although this selected volume may be highly warped with respect to the z axis, its projection with respect to the x axis is now free of metal-induced spatial shifts.
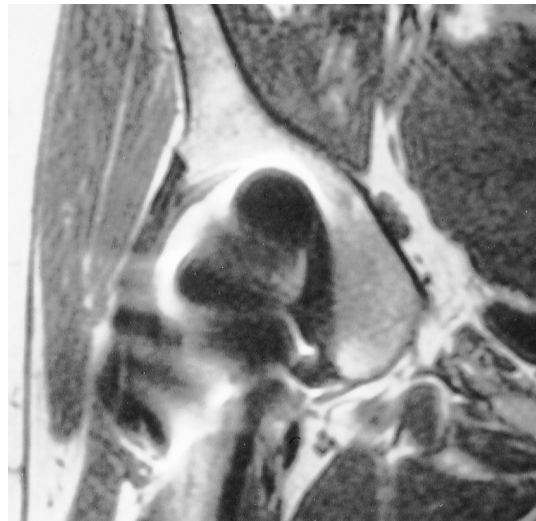
Clinical Experience

Our early clinical experience indicates that significant improvement in image quality in the presence of metal can be readily achieved by using the MARS technique in a variety of musculoskeletal imaging situations. The following examples illustrate a few of the potential clinical applications of this technique.

Hip

Femoral neck fractures are common injuries and are usually treated with stabilization techniques by using metal devices such as cannulated screws. Although satisfactory alignment can be achieved in most cases, postoperative complications are relatively common. Avascular necrosis of the femoral head is a significant and common complication and is difficult to detect with radiography, CT, or bone scintigraphy. The vascular supply to the femoral head consists of a circumflex femoral branch of the deep femoral artery as well as small vessels within the ligament of the femoral head and capsular vessels. After a fracture, some or all of this blood supply may be lost. Osteonecrosis may become clinically apparent weeks or months after the fracture, and plain radiographic findings are often unremarkable until frank collapse of the femoral head occurs. Use of MR imaging to detect early avascular necrosis of the femoral head is also problematic. Without use of a metal suppression sequence, it is often not possible to adequately visualize the marrow of the femoral head at MR imaging. In our experience, the MARS technique usually allows visualization of the subarticular marrow in the femoral head, thus allowing avascular necrosis to be diagnosed or excluded (Fig 3). This technique has proved
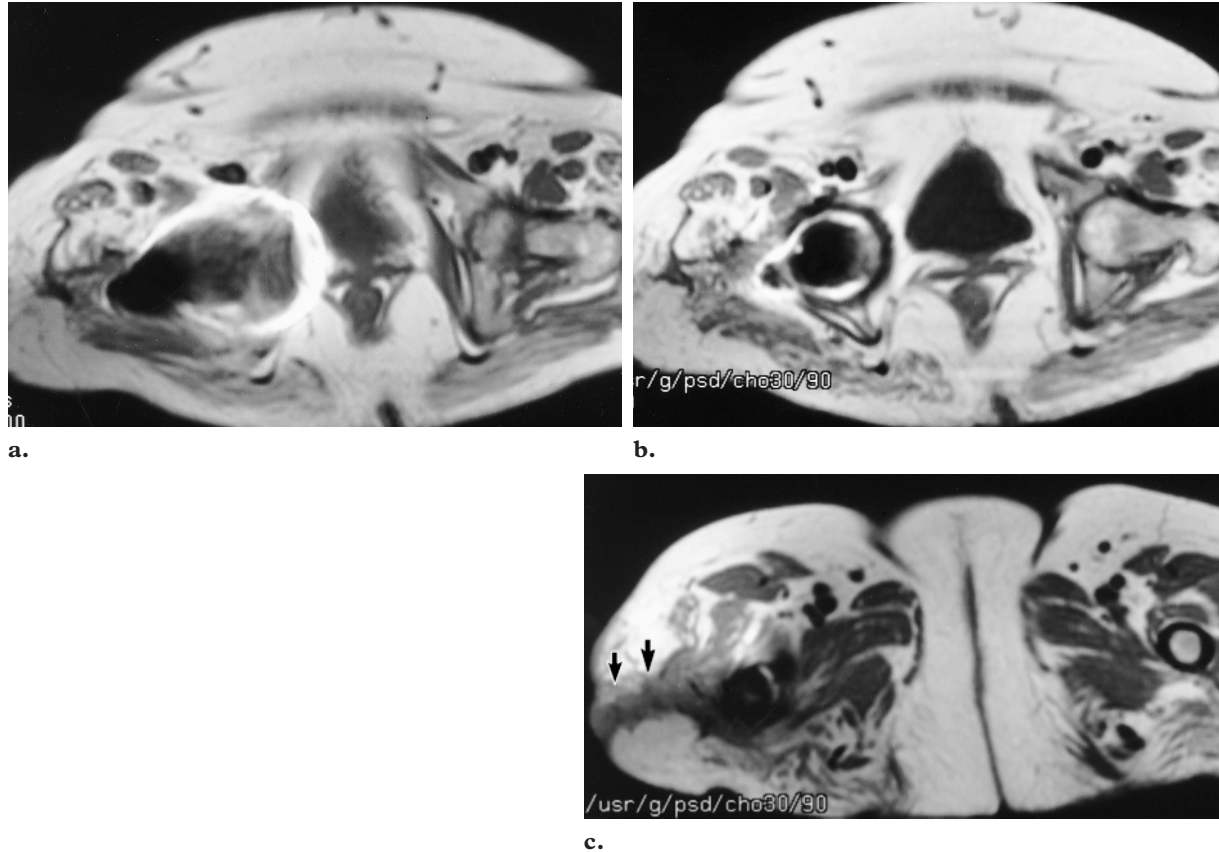
a.

b.

c.

Figure 3.   Avascular necrosis in a 56-year-old man with hip pain 4 months after a femoral neck fracture, which was transfixed with three screws. **(a)** Frog-leg radiograph of the hip shows the screws in position. The fracture is in satisfactory alignment and appears well healed. The femoral head is intact with no evidence of sclerosis or collapse. **(b)** Coronal T1-weighted spin-echo MR image (600/15) through the hip shows extensive artifact, which precludes evaluation of the femoral head and joint space. **(c)** Corresponding MR image obtained with the MARS technique shows diminished artifact. A focus of avascular necrosis is clearly seen in the superior aspect of the femoral head (arrow); this finding presumably accounted for the patient's persistent and increasing hip pain despite the normal radiographic appearance.

particularly useful in assessing patients with persistent pain after a femoral neck fracture because early diagnosis of avascular necrosis results in reduction of weight-bearing activities by the patient and decreases the likelihood of femoral head collapse and fragmentation.

The complications of hip joint replacement surgery are difficult or impossible to image with CT or conventional MR imaging. Even in the presence of such large pieces of metal, we have been

Figure 4.   Persistent drainage from the lateral aspect of the superior thigh in a 68-year-old woman 5 years after femoral hemiarthroplasty. **(a)** Axial T1-weighted spin-echo MR image (800/12) shows considerable artifact around the prosthesis. **(b)** Corresponding MR image obtained with the MARS technique shows marked reduction of artifact, thus allowing much better assessment of the surrounding soft tissues. Note that the anterior and posterior columns of the acetabulum can be readily visualized, whereas they were completely obscured on the conventional MR image **(a)**. **(c)** MR image obtained with the MARS technique several centimeters inferior to **b** shows the site of the drainage, which can be seen extending laterally in a low-signal-intensity track (arrows) traversing the higher-signal-intensity fat. No abnormal soft-tissue collection is apparent directly around the hip joint because spontaneous decompression has occurred. Note that the soft tissues of the thigh around the femoral component are well seen.
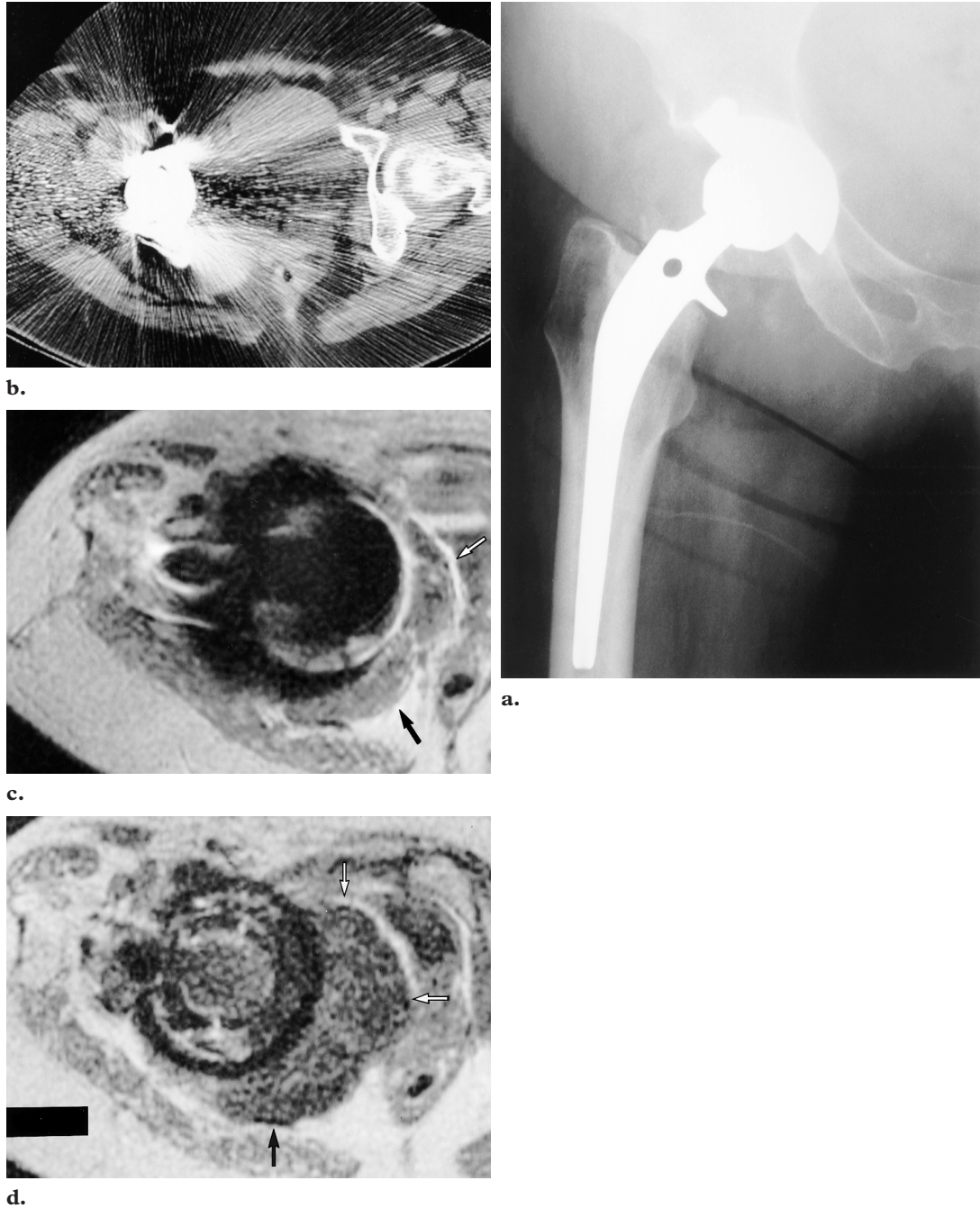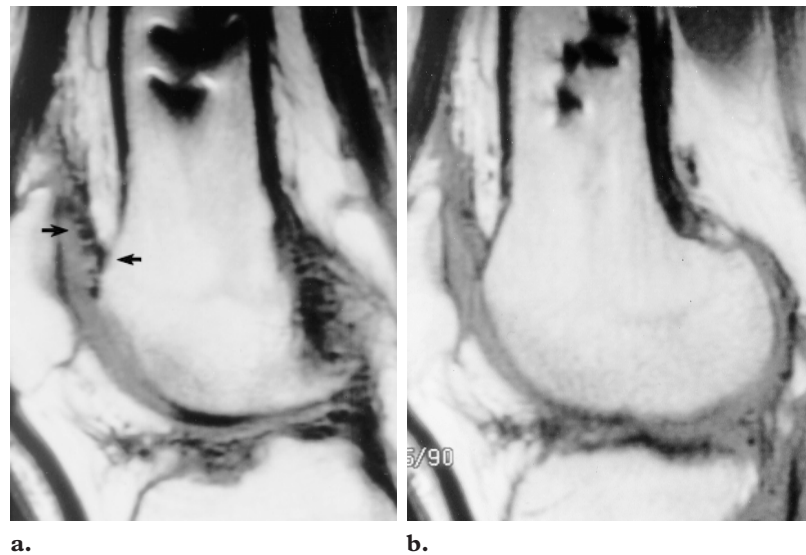

a.

b.

c.

able to significantly reduce metal artifact using the MARS technique, thus allowing assessment of the periprosthetic soft tissues (Fig 4). Such assessment has proved especially useful in patients with infected total hip arthroplasties, in whom assessment of adjacent soft-tissue inflammation or abscesses is desirable prior to surgery. Even in the presence of the arthroplasty components, abscess cavities immediately adjacent to the joint are visible. The MARS technique is also useful for postoperative assessment after resection of bone tumors and reconstruction. Many patients who undergo these procedures have metallic reconstruction components, and visualization of the adjacent soft tissue is necessary to detect early recurrent or residual tumor (Fig 5).

We have also found the MARS technique useful in localizing unopacified methyl methacrylate cement within the medullary space of both the femur and acetabulum prior to hip arthroplasty revision surgery. During surgery, the methyl methacrylate cement needs to be removed from the

Figure 5.   Recurrent synovial osteochondromatosis in an obese 50-year-old woman who underwent total hip arthroplasty 2 years earlier at the time of complete synovectomy for synovial osteochondromatosis. She presented with gradually increasing hip pain. **(a)** Anteroposterior radiograph is unremarkable. **(b)** CT scan through the hip joint is of poor quality, with marked beam hardening and spray artifact precluding adequate evaluation of the periarticular soft tissues. **(c)** Axial T1-weighted spin-echo MR image (600/15) through the hip shows extensive artifact. Although some bowing of the soft tissues medial to the hip can be seen (arrows), a discrete mass is hard to appreciate. **(d)** Corresponding MR image obtained with the MARS technique clearly shows a large soft-tissue mass (arrows). The mass, which was later diagnosed as recurrent synovial osteochondromatosis, compresses the bladder, vagina, and rectum and extends posteriorly to almost come in contact with the gluteus maximus muscle. Note that the cup liner can even be partially visualized within the joint.

a.   b.

Figure 6.   Bone staples and metallic crystals in a 36-year-old man 4 years after anterior cruciate ligament reconstruction with a hamstring tendon and an "over the top" technique (ie, stapling the cranial aspect of the neoligament to the distal femur). **(a)** Sagittal T1-weighted spin-echo MR image (500/14) clearly shows artifact from bone staples at the top of the image. In addition, numerous small areas of low signal intensity can be seen in the posterior aspect of the suprapatellar bursa (arrows), which represent small metallic crystals deposited at the time of previous surgery (these could not be seen on radiographs). **(b)** Corresponding MR image obtained with the MARS technique shows marked reduction of artifact from both bone staples and metallic crystals.

medullary cavity before new components can be installed. Therefore, preoperative localization helps the surgeon plan the site and extent of osteotomy required.

Knee
Many patients have implanted metal staples, pins, or screws adjacent to the knee joint, often as a result of previous fracture or anterior cruciate ligament reconstruction surgery. These patients may reinjure the knee and require further assessment

with MR imaging for a possible recurrent internal derangement. The MARS technique is helpful in minimizing the amount of metal artifact in these patients, thus allowing visualization of important structures (Figs 6, 7). This technique is particularly helpful in patients who have undergone anterior cruciate ligament reconstruction, especially if large interference screws were used. Even in patients who have undergone total knee arthroplasty, the MARS technique can significantly improve visualization of the periprosthetic bone and soft-tissue structures such as popliteal cysts or the posterior cruciate ligament (if a ligament-sparing prosthesis was used) (3,8) (Figs 8, 9).
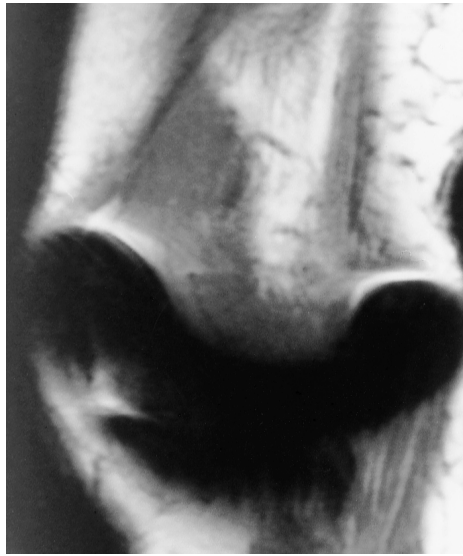
a.

b.

c.

d.

Figure 7. Ligament tear in a 34-year-old woman who had undergone two anterior cruciate ligament reconstructions. She presented with symptoms suggestive of neoligament failure. **(a)** Lateral radiograph shows two bone staples in the distal femur and an unusual wide tunnel with sclerotic margins in the anterior aspect of the superior tibia. **(b)** Sagittal gradient-echo MR image (400/14, 30° flip angle) shows marked susceptibility artifact obscuring the entire intraarticular portion of the neoligament. **(c)** Sagittal T1-weighted spin-echo MR image (400/12) clearly shows the portion of the neoligament within the osseous tunnel (straight arrow). However, metallic crystals obscure the more cranial portion (curved arrow). **(d)** Corresponding MR image obtained with the MARS technique shows reduction of artifact, thus allowing more of the ligament to be assessed. The cranial portion of the ligament is noted to be torn; this finding was confirmed at surgery.
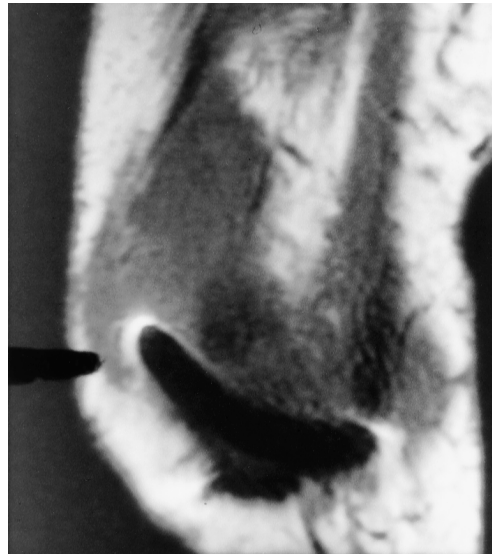
a.

Figure 8.   Normal findings in an asymptomatic 59-year-old man 2 years after tricompartment total knee arthroplasty. **(a)** Lateral radiograph is unremarkable. **(b, c)** Sagittal **(b)** and axial **(c)** T1-weighted spin-echo MR images (500/12) show large areas of signal void and distortion, as well as accompanying regions of high signal intensity. **(d, e)** Corresponding sagittal **(d)** and axial **(e)** MR images obtained with the MARS technique show dramatic reduction of artifact, thus allowing better resolution of the soft tissues adjacent to the arthroplasty. The improved resolution is especially evident on the axial image **(e)**.
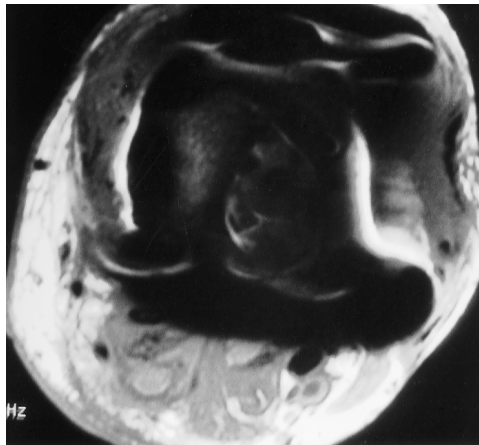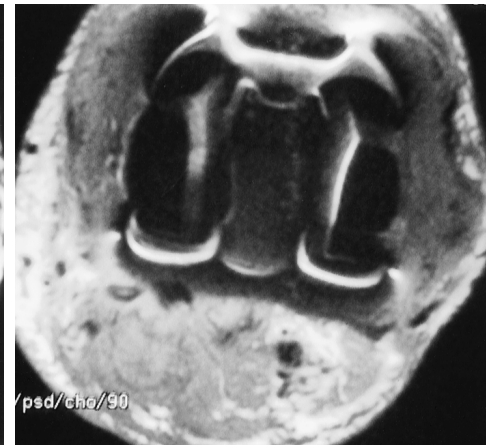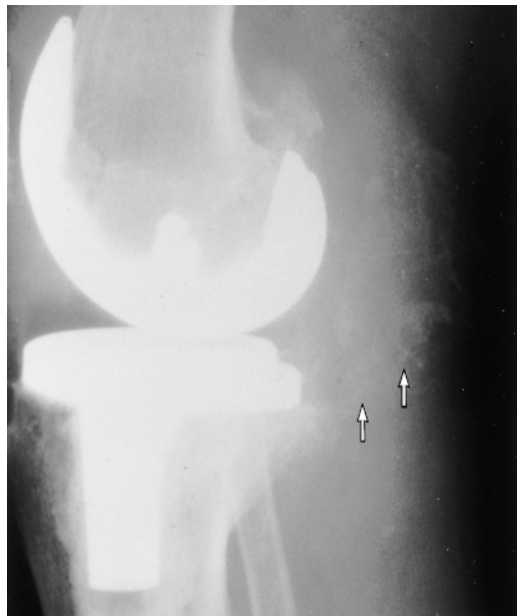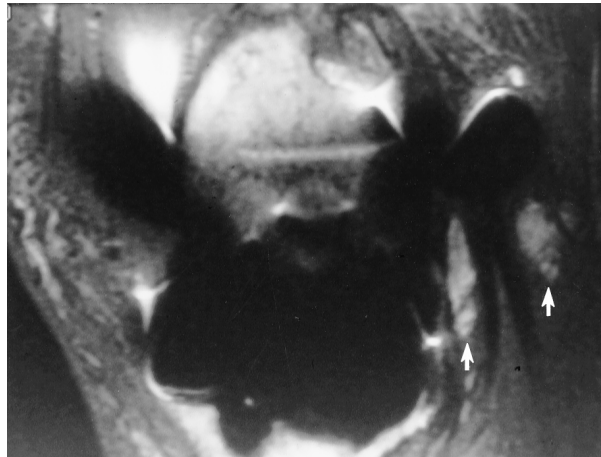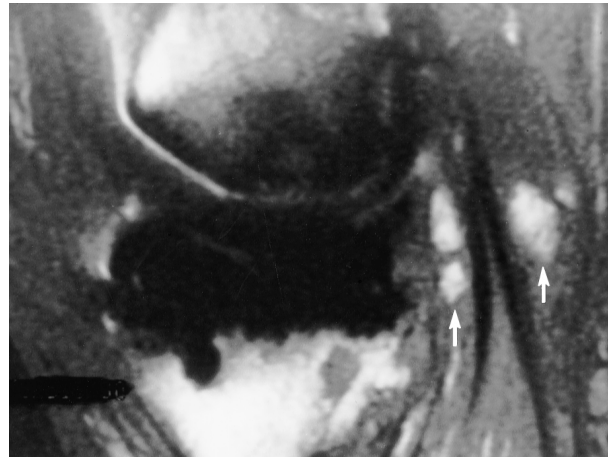

b.

d.

c.

e.

a.

Figure 9.   Multiple loose bodies within a Baker cyst in a 62-year-old man who had undergone total knee arthroplasty. **(a)** Lateral radiograph shows a knee arthroplasty with accompanying joint effusion and several slightly calcified areas of increased opacity (arrows) at the posterior aspect of the joint. **(b)** Sagittal T1-weighted spin-echo MR image (500/15) shows extensive artifact involving the metal components. At the posterior aspect of the joint, some high-signal-intensity lesions (arrows) are noted around the hamstring and gastrocnemius tendons. **(c)** Corresponding MR image obtained with the MARS technique shows greatly decreased artifact, thus allowing visualization of the high-signal-intensity fat within the marrow in the ossified loose bodies (arrows).

b.

c.

Spine

Patients with spinal fixation hardware may develop complications such as spinal cord compression, nerve root compression, vertebral instability, or infection. Evaluation in these clinical situations can be difficult because metal artifact often makes both CT and conventional MR imaging unhelpful. Standard MR imaging is difficult due to the large size of the metal devices and the proximity of the metal to the anatomic structures of concern, particularly the spinal canal and its contents (2). The MARS technique consistently decreases artifact size and intensity and significantly reduces geometric distortion (Fig 10). This technique

a.   b.   c.

Figure 10.   Vertebral displacement in a 39-year-old man who underwent posterior fixation for progressive back pain secondary to spondylolysis and spondylolisthesis. **(a)** Lateral radiograph shows the posterior fixation device extending from L4 to S1 with grade II anterior displacement of L5 over S1. **(b)** Sagittal T1-weighted spin-echo MR image (500/15) shows geometric distortion. **(c)** Corresponding MR image obtained with the MARS technique shows marked improvement in the degree of distortion.

frequently improves image quality sufficiently to allow visualization of the vertebral bodies and spinal canal contents (Fig 11) (17).

Wrist
The MARS technique can be helpful in evaluating the wrist in patients who have undergone wrist fusion (Fig 12) or Herbert screw fixation of scaphoid fractures. Reduction of the metal artifact can improve detection of avascular necrosis in the proximal pole of the scaphoid.

Current Status of Technique
In our experience, the MARS technique reliably allows improved visualization of the tissues adjacent to implanted metal devices and enables a number of new musculoskeletal MR imaging applications. This technique requires no additional imaging time and can be used in conjunction with intravenous gadolinium enhancement. We have pulse programmed the MARS technique as an

adjunct to spin-echo sequences, but in theory it can be used with any pulse sequence. The technique results in a decrease in signal intensity artifacts and geometric distortion artifacts.

The principal disadvantage of the MARS sequence is an inherent element of slight blurring, which we hope to be able to minimize in the future. Geometric distortion is also not completely suppressed, although notably reduced. Owing to the larger frequency bandwidths, the signal-to-noise ratio with the MARS technique is generally lower than with conventional sequences. The decrease in signal-to-noise ratio can be overcome by increasing the number of signals acquired at the cost of increased imaging time. At present, this technique has been developed for use with only T1-weighted sequences. The technique is not commercially available at this time.

Conclusion
The MARS technique appears to hold great promise for significantly reducing both signal void and geometric distortion surrounding metallic implants in the musculoskeletal system.
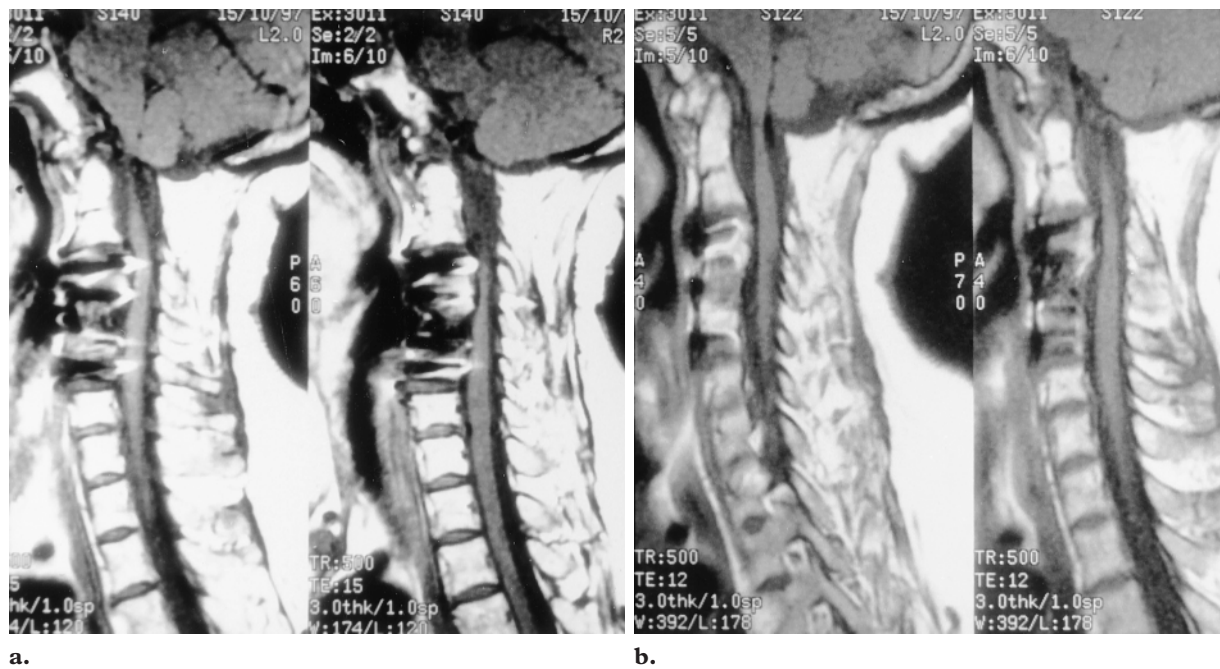
a.   **b.**

Figure 11. Anterior fixation of the cervical spine from C3 to C5 in a 74-year-old man. **(a)** Sagittal T1-weighted spin-echo MR images (500/15) show artifact produced by the screws transfixing the anterior plate. The artifact extends into the anterior aspect of the spinal canal and distorts the anterior contours of the cord. **(b)** Corresponding MR images obtained with the MARS technique (500/12) show marked improvement in the demonstration of the anterior spinal canal.
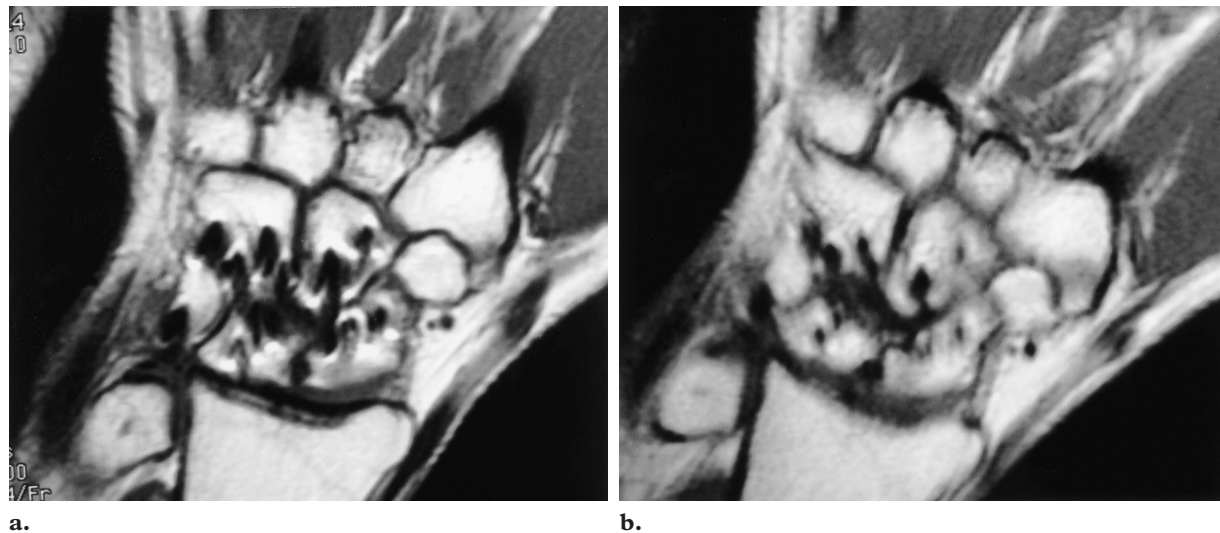

a.   **b.**

Figure 12. Normal findings in a 35-year-old man who underwent wrist fusion with multiple bone staples. **(a)** Coronal T1-weighted spin-echo MR image (400/12) shows multiple areas of artifact with distortion and poor visualization of carpal bones and joints. **(b)** Corresponding MR image obtained with the MARS technique shows some increased blurring but a dramatic reduction in distortion and improved demonstration of the bone around the midcarpal space.

References

1. Czervionke LF, Daniels DL, Wehrli FW, et al. Magnetic susceptibility artifacts in gradient-recalled echo MR imaging. AJNR Am J Neuroradiol 1988; 9:1149–1155.
2. Tartaglino LM, Flanders AE, Vinitski S, Friedman DP. Metallic artifacts on MR images of the postoperative spine: reduction with fast spin-echo techniques. Radiology 1994; 190:565–569.
3. Shellock FG, Mink JH, Curtin S, Friedman MJ. MR imaging and metallic implants for anterior cruciate ligament reconstruction: assessment of ferromagnetism and artifact. J Magn Reson Imaging 1992; 2:225–228.
4. Heindel W, Friedman G, Bunke J, Thomas B, Firsching R, Ernestus RI. Artifacts in MR imaging after surgical intervention. J Comput Assist Tomogr 1986; 10:596–599.
5. Laakman RW, Kaufman B, Han JS, et al. MR imaging in patients with metallic implants. Radiology 1985; 157:711–714.
6. Bellon EM, Haacke EM, Coleman PE, Sacco DC, Steiger DA, Gangarosa RE. MR artifacts: a review. AJR Am J Roentgenol 1986; 147:1271–1281.
7. Eustace S, Hernan J, Goldberg R, et al. A comparison of conventional spin-echo and turbo spin-echo imaging of soft tissues adjacent to orthopedic hardware. AJR Am J Roentgenol 1998; 170:455–458.
8. Eustace S, Goldberg R, Williamson D, et al. MR imaging of soft tissues adjacent to orthopaedic hardware: techniques to minimize susceptibility artifact. Clin Radiol 1997; 52:589–594.
9. Petersilge CA, Lewin JS, Duerk JL, Yoo JU, Ghaneyem AJ. Optimizing imaging parameters for MR evaluation of the spine with titanium pedicle screws. AJR Am J Roentgenol 1996; 166:1213–1218.
10. Törmänen J, Tervonen O, Koivula A, Junila J, Suramo I. Image technique optimization in MR imaging of a titanium alloy joint prosthesis. J Magn Reson Imaging 1996; 6:805–811.
11. Farahani K, Sinha U, Sinha S, Chiu LCL, Lufkin RB. Effect of field strength on susceptibility artifacts in magnetic resonance imaging. Comput Med Imaging Graph 1990; 14:409–413.
12. Suh JS, Jeong EK, Shin KH, et al. Minimizing artifacts caused by metallic implants at MR imaging: experimental and clinical studies. AJR Am J Roentgenol 1998; 171:1207–1213.
13. Rupp R, Ebraheim NA, Savolaine ER, Jackson WT. Magnetic resonance imaging evaluation of the spine with metal implants. Spine 1993; 18:379–385.
14. Ebraheim NA, Savolaine ER, Zeiss J, Jackson WT. Titanium hip implants for improved magnetic resonance and computed tomography examinations. Clin Orthop 1992; 275:194–198.
15. Frazzini VI, Kagetsu NJ, Johnson CE, Destian S. Internally stabilized spine: optimal choice of frequency-encoding gradient direction during MR imaging minimizes susceptibility artifact from titanium vertebral body screws. Radiology 1997; 204:268–272.
16. McGowan AJ, MacKay AL, Xiang QS, Connell DG, Janzen DL, Munk PL. Reduction of image distortion in the presence of metal (abstr). Proceedings of the Fifth Meeting of the International Society for Magnetic Resonance in Medicine. Berkeley, Calif: International Society for Magnetic Resonance in Medicine, 1997; 1973.
17. Chang SD, Janzen DL, Sallomi DF, Munk PL. MRI of spinal hardware: comparison of conventional T1-weighted sequence with a new metal artifact reduction sequence (abstr). Radiology 1998; 209(P):614.
18. Olsen RV, Janzen DL, Sallomi DF, Munk PL, MacKay AL, Xiang QS. Clinical application of a new method of metal artifact suppression on MR imaging (abstr). Radiology 1998; 209(P):612.
19. Cho ZH, Kim DJ, Kim YK. Total inhomogeneity correction including chemical shifts and susceptibility by view angle tilting. Med Phys 1988; 15:7–11.